because EUS-HGS with a covered metal stent has the potential to cause segmental cholangitis and liver abscesses because of blockage of the bile stream. Indeed, we have experienced these conditions. Second, stent patency is not so long[1] and stent occlusion is sometimes frequent with EUS-HGS. If the covered metal stent of EUS-HGS is occluded by debris or bile stones, complete stone removal through the EUS-HGS is very difficult. If stone removal through the EUS-HGS is attempted, it is easy for the stones to get pushed into a bile duct branch. Hence, we sometimes have no choice but to insert an antegrade stent to push out the stones. Unlike EUS-HGS, which has the advantage of no possibility of causing pancreatitis, antegrade drainage can cause pancreatitis; hence, antegrade drainage through Vater's papilla has limited utility. Therefore, stent placement with EUS-HGS is also associated with several clinical problems.

In conclusion, EUS-BD is certainly a useful procedure, the utility of which is likely to increase with the development of newer techniques and devices. However, at present, these procedures carry the risk of major technical and clinical problems. This fact must always be kept in mind when prescribing these procedures. Further, as the occurrence of complications is closely related to the devices used, special new devices should be developed to minimize the risk of complications.

Authors declare no conflict of interests for this article.

Kazuo Hara and Kenji Yamao
Department of Gastroenterology, Aichi Cancer Center Hospital, Nagoya, Japan
doi: 10.1111/den.12201

REFERENCES

1 Park DH, Jang JW, Lee SS, Seo DW, Lee SK, Kim MH. EUS-guided biliary drainage with transluminal stenting after failed ERCP: Predictors of adverse events and long-term results. *Gastrointest. Endosc.* 2011; **74**: 1276–84.
2 Hara K, Yamao K, Hijioka S *et al.* Prospective clinical study of endoscopic ultrasound-guided choledochoduodenostomy with direct metallic stent placement using a forward-viewing echoendoscope. *Endoscopy* 2013; **45**: 392–6.
3 Hara K, Yamao K, Niwa Y *et al.* Prospective clinical study of EUS-guided choledochoduodenostomy for malignant lower biliary tract obstruction. *Am. J. Gastroenterol.* 2011; **106**: 1239–45.
4 Vila JJ, Pérez-Miranda M, Vazquez-Sequeiros E *et al.* Initial experience with EUS-guided cholangiopancreatography for biliary and pancreatic duct drainage: A Spanish national survey. *Gastrointest. Endosc.* 2012; **76**: 1133–41.
5 Martins F, Rossini L, Ferrari A. Migration of a covered metallic stent following endoscopic ultrasound-guided hepaticogastrostomy: Fatal complication. *Endoscopy* 2010; **42** (S 02): E126–7.

Pancreatology 14 (2014) 221–226

Contents lists available at ScienceDirect

Pancreatology

journal homepage: www.elsevier.com/locate/pan

Original article

Ring-enhancement pattern on contrast-enhanced CT predicts adenosquamous carcinoma of the pancreas: A matched case-control study

Hiroshi Imaoka [a,*], Yasuhiro Shimizu [b], Nobumasa Mizuno [a], Kazuo Hara [a], Susumu Hijioka [a], Masahiro Tajika [a], Tsutomu Tanaka [a], Makoto Ishihara [a], Takeshi Ogura [a], Tomohiko Obayashi [a], Akihide Shinagawa [a], Masafumi Sakaguchi [a], Hidekazu Yamaura [c], Mina Kato [c], Yasumasa Niwa [a], Kenji Yamao [a]

[a] Department of Gastroenterology, Aichi Cancer Center Hospital, Nagoya, Japan
[b] Department of Gastroenterological Surgery, Aichi Cancer Center Hospital, Nagoya, Japan
[c] Department of Diagnostic and Interventional Radiology, Aichi Cancer Center Hospital, Nagoya, Japan

ARTICLE INFO

Article history:
Received 14 August 2013
Received in revised form
2 February 2014
Accepted 16 February 2014
Available online 25 February 2014

Keywords:
Adenosquamous carcinoma of the pancreas (ASC)
Pancreatic ductal adenocarcinoma (PDAC)
Contrast-enhanced computed tomography (CT)
Endoscopic ultrasonography (EUS)
Matched case-control study

ABSTRACT

Objectives: Adenosquamous carcinoma of the pancreas (ASC) is a rare malignant neoplasm of the pancreas, exhibiting both glandular and squamous differentiation. However, little is known about its imaging features. This study examined the imaging features of pancreatic ASC.
Methods: We evaluated images of contrast-enhanced computed tomography (CT) and endoscopic ultrasonography (EUS). As controls, solid pancreatic neoplasms matched in a 2:1 ratio to ASC cases for age, sex and tumor location were also evaluated.
Results: Twenty-three ASC cases were examined, and 46 solid pancreatic neoplasms (43 pancreatic ductal adenocarcinomas, two pancreatic neuroendocrine tumors and one acinar cell carcinoma) were matched as controls. Univariate analysis demonstrated significant differences in the outline and vascularity of tumors on contrast-enhanced CT in the ASC and control groups ($P < 0.001$ and $P < 0.001$, respectively). A smooth outline, cystic changes, and the ring-enhancement pattern on contrast-enhanced CT were seen to have significant predictive powers by stepwise forward logistic regression analysis ($P = 0.044$, $P = 0.010$, and $P = 0.001$, respectively). Of the three, the ring-enhancement pattern was the most useful, and its predictive diagnostic sensitivity, specificity, positive predictive value and negative predictive value for diagnosis of ASC were 65.2%, 89.6%, 75.0% and 84.3%, respectively.
Conclusions: These results demonstrate that presence of the ring-enhancement pattern on contrast-enhanced CT is the most useful predictive factor for ASC.

1. Introduction

Adenosquamous carcinoma of the pancreas (ASC) is a variant of pancreatic ductal adenocarcinoma (PDAC), exhibiting both glandular and squamous differentiation [1–4]. ASC accounts for 3–4% of malignant neoplasms of the pancreas, and is reportedly more aggressive than conventional PDAC, with simultaneous metastases to the liver and lymph nodes being seen more frequently among ASC patients [5,6]. Although diagnosis of ASC is important for predicting the prognosis of patients, recognition of ASC is not easy. One reason for this is that the clinical characteristics of ASC remain unclear because of its rarity. Since most descriptions of ASC have been from case studies and small surgical series [7], its imaging features have not yet been proposed. This study examined the imaging features of ASC in a matched case-control study.

2. Methods

The institutional review board of the hospital approved this study. We evaluated the pathological and clinical records of ASC

* Corresponding author. Department of Gastroenterology, Aichi Cancer Center Hospital, 1-1 Kanokoden, Chikusa-ku, Nagoya, Aichi 464-8681, Japan. Tel.: +81 52 7626111; fax: +81 52 7635233.
E-mail address: hiroshi.imaoka.md@me.com (H. Imaoka).

http://dx.doi.org/10.1016/j.pan.2014.02.005
1424-3903/

and pancreatic neoplasm patients treated at our institution between 2001 and 2012. All cases were diagnosed based on cytological or histological confirmation from surgical specimens or endoscopic ultrasound-guided fine-needle aspiration (EUS-FNA), and only cases in whom imaging data of both contrast-enhanced computed tomography (CT) and endoscopic ultrasonography (EUS) were available were included in this study. The criteria for pathological diagnosis of ASC have been previously described [1,8]. Patients with a history of squamous cell carcinoma or other cancers were excluded from this analysis, to distinguish between primary ASC and metastasis from other sites [9].

Patients were evaluated by EUS using a GF-UCT240 convex array echoendoscope (Olympus Optical Co. Ltd., Tokyo, Japan), and EUS-FNA was performed after EUS examination, as previously described [10,11].

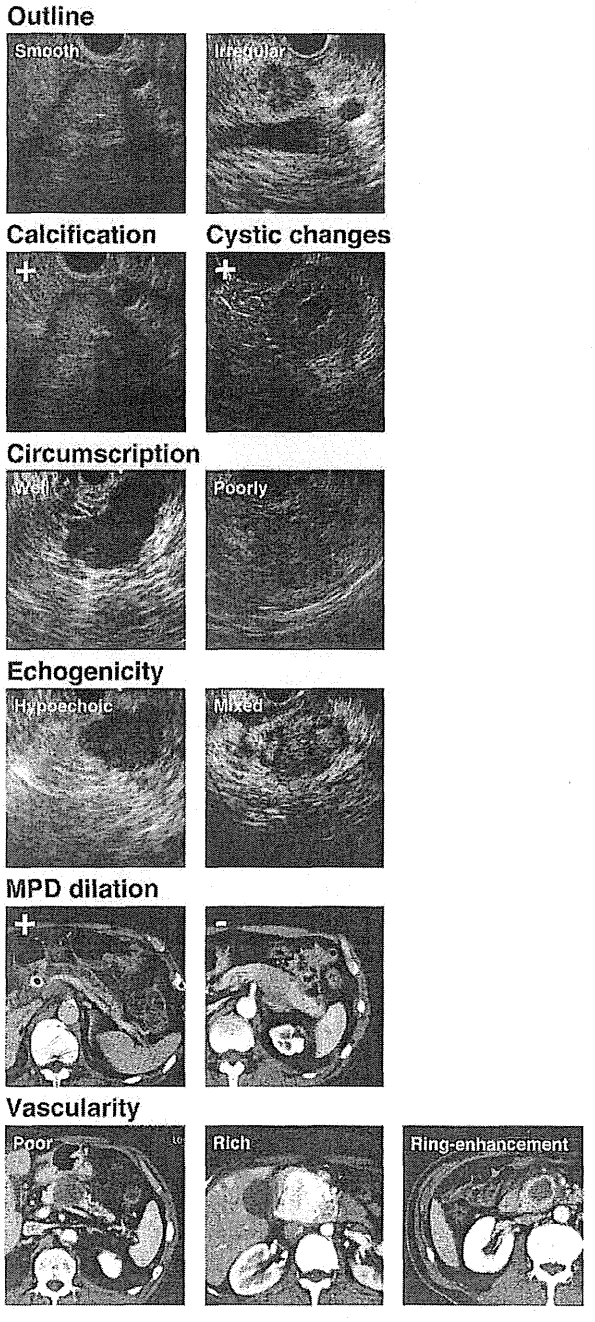

Fig. 1. Representative examples of the imaging parameters.

As controls, cases with solid pancreatic neoplasms, matched in a 2:1 ratio to ASC cases for age (±3 years), sex and tumor location, were also included in this study. Data were abstracted from medical records by 2 reviewers (T.O., T.O.) who were blinded to case-control status. Two reviewers independently assessed these data, and disagreements were resolved by discussion with a third reviewer (K.Y.).

Images of contrast-enhanced CT were reviewed by two blinded radiologists (K.Y., M.K.), and that of EUS were evaluated by two experienced endosonographers (A.S., M.S.). All the evaluators were blind to the patients' pathological and clinical data, which they independently assessed in a random order. Any disagreements were resolved by discussion with a fifth reader (K.Y.). The imaging data were evaluated for the following 7 parameters: outline (smooth vs. irregular), calcification, cystic changes, circumscription (well vs. poorly circumscribed), echogenicity (hyperechoic, hypoechoic and mixed pattern), main pancreatic duct (dilated vs. not dilated), and vascularity (poor, rich and ring-enhancement). We defined the main pancreatic duct as being dilated if it was greater than 2 mm in diameter. In addition, the ring-enhancement pattern was defined as an area of decreased density surrounded by a bright thin rim due to concentration of the contrast-enhancing dye. Representative images are shown in Fig. 1. Five of the 7 parameters (outline, calcification, cystic changes, circumscription and echogenicity) were evaluated on EUS images, while 5 parameters (outline, calcification, cystic changes, main pancreatic duct, and vascularity) were evaluated on contrast-enhanced CT images.

3. Statistical analysis

To compare the patients' backgrounds between ASC and control groups, univariate analysis was performed using the Student's *t*-test for continuous variables, and chi-square test or Fisher's exact test for categorical variables. To compare the various imaging findings between ASC and control groups, univariate analysis was performed using the chi-square test or Fisher's exact test for categorical variables. Multivariate analysis was performed to assess the independent effects of imaging parameters in predicting the diagnosis of ASC using a stepwise forward logistic regression analysis. The likelihood ratio test was used to assess the statistical significance of the variables for the final model. The sensitivity, specificity, positive predictive value (PPV) and negative predictive value (NPV) for diagnosis of ASC were indicated by 95% confidence intervals (CI).

For assessment of interobserver variability of categorical imaging findings, a κ analysis was performed. The levels of agreement were defined as: no agreement ($\kappa < 0$), slight agreement ($\kappa = 0.00$—

Table 1
Baseline characteristics of the patients.

	ASC ($N = 23$)	Control ($N = 46$)	*P*-value
Age (yr)			
	63.26 ± 8.30	62.43 ± 9.06	0.715[a]
Sex			
Male (%)	15 (65.21)	30 (65.21)	
Female (%)	8 (34.78)	16 (34.78)	1.000[b]
Tumor location			
Head (%)	10 (43.47)	20 (43.47)	
Body-Tail (%)	13 (56.52)	26 (56.52)	1.000[b]
Size (mm)	41.26 ± 14.56	36.00 ± 17.54	0.234[a]
CEA (ng/ml)	38.44 ± 85.32	76.10 ± 273.48	0.539[a]
CA19-9 (U/ml)	16,094.10 ± 53,959.46	7931.90 ± 20,165.07	0.485[a]

ASC, adenosquamous carcinoma; yr, years; SD, standard deviation.
[a] Student's *t*-test.
[b] Chi-square test.

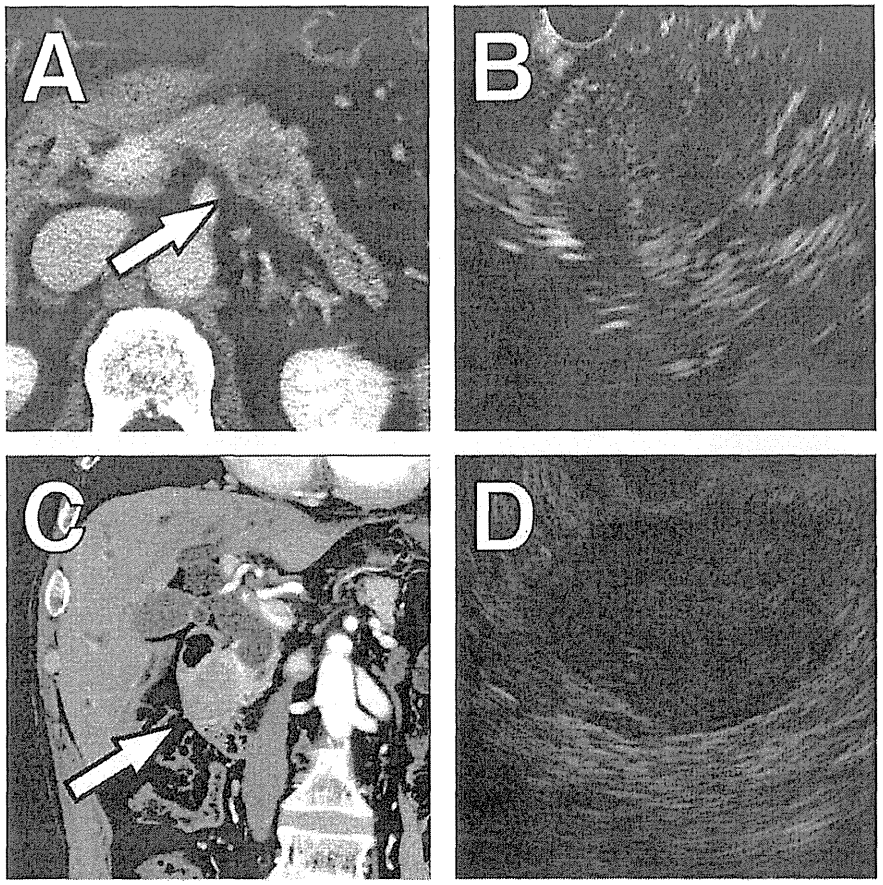

Fig. 2. Representative images of control cases. Pancreatic ductal adenocarcinoma. (A) Contrast-enhanced CT showed a hypodense tumor in the body of the pancreas with pancreatic duct dilatation (white arrow), and (B) EUS showed a mixed-echoic mass with an irregular border. Pancreatic neuroendocrine tumor. (C) Contrast-enhanced CT showed a hyperdense tumor in the head of the pancreas (white arrow), and (D) EUS showed a well-circumscribed hypoechoic mass.

0.20), fair agreement (κ = 0.21–0.40), moderate agreement (κ = 0.41–0.60), substantial agreement (κ = 0.61–0.80), and almost perfect agreement (κ = 0.81–1.00) [12].

All values represent mean ± standard deviation. Values of $P < 0.05$ were considered statistically significant and all P values were two-sided. Data were analyzed using STATA version 11.1 statistical software (StataCorp, College Station, TX, USA).

4. Results

Of the 996 patients with pancreatic neoplasms treated at our hospital between 2001 and 2012, a total of 34 cases of ASC were identified, 23 of who met the inclusion criteria. Of them, 5 patients were diagnosed based on surgical findings, and the others were diagnosed based on EUS-FNA findings. The patients' characteristics are summarized in Table 1. Mean age at diagnosis was 63.26years (range, 44–79 years). Males were affected more frequently than females. Ten of these cases (43.47%) were located in the pancreatic head and the others were in the pancreatic body-tail. The characteristics of the control group in the matched case-control study are also shown in Table 1. Details of the control group were as follows: pancreatic ductal adenocarcinoma (PDAC) in 43 cases, pancreatic neuroendocrine tumor (PNET) in 2 cases and acinar cell carcinoma (ACC) in 1 case. Representative images of control cases (PDAC and PNET) are shown in Fig. 2. Although the tumor size tended to be larger in ASC than in control patients, the difference was not statistically significant.

The differences in the imaging parameters between the two groups are shown in Table 2. Of them, two imaging findings were statistically significantly different between ASC and control groups. A smooth outline of the tumor on contrast-enhanced CT was seen more frequently in ASC than control group patients ($P < 0.001$). Further, vascularity of the tumor on contrast-enhanced CT showed significant differences between ASC and control groups ($P < 0.001$). The ring-enhancement pattern of the tumor tended to be seen more frequently in the ASC than the control group. With regard to interobserver agreement in categorical imaging findings, κ values demonstrated substantial agreement for EUS (0.69) and almost perfect agreement for contrast-enhanced CT (0.90).

The results of stepwise forward logistic regression analysis with the diagnosis of ASC and control as dependent variables and the imaging parameters as independent variables are shown in Table 3. Of them, a smooth outline, cystic changes, and the ring-enhancement pattern on contrast-enhanced CT were identified as significant predictive signs. Further, the likelihood ratio test showed that these 3 parameters were statistically significant in predicting ASC ($P = 0.025$, $P = 0.003$, and $P < 0.001$, respectively). In discriminating ASC from other solid pancreatic neoplasms, the predictive diagnostic sensitivity, specificity, PPV and NPV of a smooth outline on contrast-enhanced CT were 43.5%, 93.5%, 76.9% and 76.8%, respectively, and those of cystic changes on

Table 2
Differences in the imaging parameters between adenosquamous carcinoma and control groups.

		ASC ($N = 23$)	Control ($N = 46$)	P-value
Outline				
CT	Smooth	10	3	
	Irregular	13	43	<0.001[a]
EUS	Smooth	7	5	
	Irregular	16	41	0.088[a]
Calcification				
CT	+	2	2	
	−	21	44	0.596[a]
EUS	+	1	4	
	−	22	42	0.658[a]
Cystic changes				
CT	+	8	9	
	−	15	37	0.167[b]
EUS	+	6	7	
	−	17	39	0.334[a]
Circumscription				
EUS	Well	19	33	
	Poor	4	13	0.323[b]
Echogenicity				
EUS	Hyperechoic	1	1	
	Hypoechoic	10	20	
	Mixed	12	25	0.877[b]
Main pancreatic duct				
CT	Dilated	13	27	
	Not dilated	10	19	0.863[b]
Vascularity				
CT	Poor	8	37	
	Rich	0	4	
	Ring-enhancement	15	5	<0.001[b]

[a] Fisher's exact test.
[b] Chi-square test.

contrast-enhanced CT were 34.8%, 80.4%, 47.1% and 71.2%, respectively. The ring-enhancement pattern was the most useful predictive parameter, and its predictive diagnostic sensitivity, specificity, PPV and NPV were 65.2%, 89.6%, 75.0% and 84.3%, respectively (Table 4).

The surgically resected specimens were soft, fleshy and circumscribed. A representative case is shown in Fig. 3. The tumor was encapsulated by fibrous tissue. Histological assessment of the resected specimen revealed both glandular and squamous differentiation intimately admixed. Neoplastic cells admixed with numerous delicate vessels were present at the margin of the tumor, and extensive tumor necrosis was seen at the center of the tumor. These histological patterns were seen in 80% of the cases.

Table 3
The results of stepwise forward logistic regression analysis of the 7 imaging parameters, to determine their predictive ability for adenosquamous carcinoma.

		Coefficient (β)	95% confidence interval	P-value	Odds ratio
Smooth outline	**CT[a]**	**2.362**	**0.059–4.665**	**0.044**	**10.618**
	EUS	2.361	−0.251–4.974	0.076	10.608
Calcification	CT	0.528	−2.267–3.324	0.711	1.696
	EUS	0.357	−2.606–3.321	0.813	1.429
Cystic changes	**CT[b]**	**2.969**	**0.701–5.238**	**0.010**	**19.488**
	EUS	−2.600	−5.236–0.035	0.053	0.074
Well circumscribed	EUS	−0.988	−3.030–1.053	0.343	0.372
Main pancreatic duct dilatation	CT	1.763	−0.162–3.690	0.073	5.833
Hypoechogenicity	EUS	1.241	−4.586–7.068	0.676	3.460
Mixed echogenicity	EUS	0.459	−5.315–6.234	0.876	1.583
Ring-enhancement	**CT[c]**	**3.862**	**1.504–6.220**	**0.001**	**47.570**

[a] Likelihood-ratio test; P-value; 0.025.
[b] Likelihood-ratio test; P-value; 0.003.
[c] Likelihood-ratio test; P-value; < 0.001.

5. Discussion

ASC is a malignant neoplasm of the pancreas, exhibiting both glandular and squamous differentiation. ASC is considered a variant of PDAC, accounting for 3–4% of malignant neoplasms of the pancreas [2–4]. It is considered to have a poor prognosis due to its aggressive behavior [13–15]. Boyd et al. described in their population-based analysis that overall survival (OS) following surgical resection of ASC is significantly worse as compared to that after resection of PDAC [5]. We also previously clarified that ASC is more aggressive than conventional PDAC in a matched case-control study [6]. In that study, median OS was significantly worse for ASC (8.38 months) than for PDAC (15.75 months; hazard ratio, 1.94), and simultaneous metastases to the liver and lymph nodes were seen more frequently in the ASC group than in the PDAC group. Clinically, diagnosis of ASC is important for predicting the prognosis of patients, although recognition of ASC is not easy. One reason for this is that little is known about the imaging features of ASC because of its rarity. This study, therefore, examined the imaging features of ASC in a matched case-control study.

In the matching process, control cases were carefully selected from among patients with solid pancreatic neoplasms by two blinded reviewers, the cases comprising 43 PDAC patients (93.4%), 2 PNET patients (4.3%), and 1 ACC patient (2.1%). Reportedly, the incidence of PDAC, PNET and ACC is about 90%, 2% and 1–2% of pancreatic neoplasms, respectively [16–19]. Our control group makeup was, thus, consistent with the reported incidence of each type of pancreatic neoplasm. This indicates the adequacy of our matching process.

Two of the imaging parameters, namely tumor outline and ring-enhancement pattern on contrast-enhanced CT, were seen more frequently in ASCs. Furthermore, stepwise forward logistic regression analysis demonstrated that a smooth outline, cystic changes, and the ring-enhancement pattern on contrast-enhanced CT were significant predictive signs of ASC. Pathologically, the tumor was encapsulated by fibrous tissue. Viable neoplastic cells with numerous delicate vessels were present at the margins of the tumor, and prominent necrosis was seen at the center. Thus, a smooth outline, cystic changes, and the ring-enhancement pattern on contrast-enhanced CT may reflect these pathological findings. The ring-enhancement pattern was the most useful imaging parameter, with a predictive diagnostic sensitivity and specificity in discriminating ASC from other solid pancreatic neoplasms of 65.2% and 89.6%, respectively. The diagnostic sensitivity of the ring-enhancement pattern for ASC, on the other hand, was relatively modest. This could be because several cases of ASC resembled conventional PDAC on contrast-enhanced CT images. We speculate that visualization of the pattern may depend on the degree of necrosis within the tumor. On the other hand, the PPV for ASC was 75.0%, which is a satisfactory result. This finding is important, since presence of the ring-enhancement pattern indicates a poor prognosis for patients. Once a diagnosis of ASC is made, newer chemotherapeutic regimens, such as gemcitabine + erlotinib [20] and FOLFIRINOX [21], can be attempted.

In this study, we used a combination of CT and EUS to examine imaging features of ASC using a matched case-control design. Use of this combination seems reasonable since CT and EUS are widely accepted as the most accurate imaging modalities in the diagnosis of pancreatic tumors. In a comparative study of CT and EUS, the sensitivity of CT was reported as 86% and that of EUS was reportedly 98–100% [22,23]. EUS is superior to CT for tumor and nodal staging of pancreatic cancers, while CT can identify distant non-nodal metastases more accurately than EUS [24,25]. Furthermore, the two imaging modalities complement each other during decision-making regarding therapeutic strategies in patients with

Table 4
Diagnostic sensitivity, specificity and predictive value of imaging parameters in the diagnosis of ASC.

	Sensitivity (95% CI)	Specificity (95% CI)	(Sensitivity + Specificity)/2 (95% CI)	PPV (95% CI)	NPV (95% CI)
Smooth outline (CT)	43.5% (23.2%–65.5%)	93.5% (82.1%–98.6%)	0.685 (0.575–0.794)	76.9% (46.2%–95.0%)	76.8% (63.6%–87.0%)
Cystic changes (CT)	34.8% (16.4%–57.3%)	80.4% (66.1%–90.6%)	0.576 (0.461–0.691)	47.1% (23.0%–72.2%)	71.2% (56.9%–82.9%)
Ring-enhancement	65.2% (42.7%–83.6%)	89.6% (77.3%–96.5%)	0.774 (0.665–0.883)	75.0% (50.9%–91.3%)	84.3% (71.4%–93.0%)

CI, confidence interval; PPV, positive predictive value; NPV, negative predictive value.

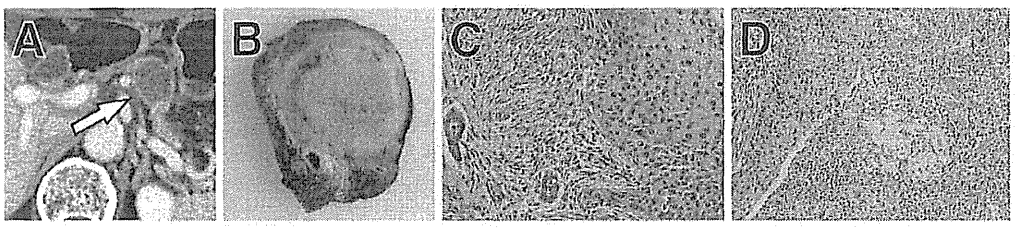

Fig. 3. Representative images of adenosquamous carcinoma (ASC) of the pancreas. (A) Contrast-enhanced CT showed a circumscribed mass in the pancreas (white arrow). The mass exhibited the ring-enhancement pattern. (B) Macroscopically, the resected tumor was soft, fleshy and circumscribed. (C) Microscopically, both glandular and squamous differentiation were present at the margins of the tumor (hematoxylin and eosin stain, original magnification ×400), and (D) extensive tumor necrosis was seen at the center of the tumor (hematoxylin and eosin stain, original magnification ×200).

pancreatic cancer. Soriano et al. reported that the accuracy of diagnosis of pancreatic tumor resectability was maximized and costs were minimized when either CT or EUS was performed initially, followed by the other test [26]. Tierney et al. suggested that although CT should be performed first, EUS should also be used because of its improved detection of vascular invasion [27].

Although EUS is a fairly sensitive modality for assessing pancreatic lesions, as previously described, a drawback of EUS is the relatively modest interobserver agreement in the interpretation of EUS findings, even by expert endosonographers. Wallace et al. reported moderate agreement (kappa = 0.45) in their examination of interobserver agreement of EUS findings for the diagnosis of chronic pancreatitis [28]. Topazian et al. reported fair to poor interobserver agreement for the interpretation of pancreatic EUS findings in familial pancreatic cancer kindreds. Furthermore, agreement was not improved by consensus [29]. On the other hand, contrast-enhanced CT is regarded as an objective imaging modality for the diagnosis of pancreatic lesions. In one study, almost perfect interobserver agreement was obtained for the assessment of CT findings in patients with pancreatic cancer (kappa >0.80) [30]. Our study, showing κ values of EUS indicating substantial agreement between the two readers (0.69), and that of CT indicating almost perfect agreement (0.90), yielded similar results to these previous studies. However, in our predictive model, the ring-enhancement pattern on contrast-enhanced CT was selected as the best predictive sign of ASC. We believe that this result might be widely acceptable.

In summary, we examined the imaging features of ASC using a matched case-control study. The present results show that presence of a ring-enhancement pattern on contrast-enhanced CT is the most useful predictive sign of ASC. In the detection and staging of pancreatic cancer, observation of a ring-enhancement pattern can indicate a poor prognosis for these patients.

Acknowledgments

The authors have no conflicts of interest to disclose.

References

[1] Hruban RH, Pitman MB, Klimstra DS. Tumors of the pancreasIn AFIP atlas of tumor pathology, 4th series, fascicle 6. Washington, DC: American Registry of Pathology; 2007.
[2] Ishikawa O, Matsui Y, Aoki I, Iwanaga T, Terasawa T, Wada A. Adenosquamous carcinoma of the pancreas: a clinicopathologic study and report of three cases. Cancer 1980;46:1192–6.
[3] Madura JA, Jarman BT, Doherty MG, Yum MN, Howard TJ. Adenosquamous carcinoma of the pancreas. Arch Surg 1999;134:599–603.
[4] Morohoshi T, Held G, Kloppel G. Exocrine pancreatic tumours and their histological classification. A study based on 167 autopsy and 97 surgical cases. Histopathology 1983;7:645–61.
[5] Boyd CA, Benarroch-Gampel J, Sheffield KM, Cooksley CD, Riall TS. 415 patients with adenosquamous carcinoma of the pancreas: a population-based analysis of prognosis and survival. J Surg Res 2012;174:12–9.
[6] Imaoka H, Shimizu Y, Mizuno N, Hara K, Hijioka S, Tajika M, et al. Clinical characteristics of adenosquamous carcinoma of the pancreas: a matched case-control study. Pancreas 2014;43:287–90.
[7] Voong KR, Davison J, Pawlik TM, Uy MO, Hsu CC, Winter J, et al. Resected pancreatic adenosquamous carcinoma: clinicopathologic review and evaluation of adjuvant chemotherapy and radiation in 38 patients. Hum Pathol 2010;41:113–22.
[8] Rahemtullah A, Misdraji J, Pitman MB. Adenosquamous carcinoma of the pancreas: cytologic features in 14 cases. Cancer 2003;99:372–8.
[9] Itani KM, Karni A, Green L. Squamous cell carcinoma of the pancreas. J Gastrointest Surg 1999;3:512–5.
[10] Imaoka H, Yamao K, Bhatia V, Shimizu Y, Yatabe Y, Koshikawa T, et al. Rare pancreatic neoplasms: the utility of endoscopic ultrasound-guided fine-needle aspiration – a large single center study. J Gastroenterol 2009;44:146–53.
[11] Haba S, Yamao K, Bhatia V, Mizuno N, Hara K, Hijioka S, et al. Diagnostic ability and factors affecting accuracy of endoscopic ultrasound-guided fine needle aspiration for pancreatic solid lesions: Japanese large single center experience. J Gastroenterol 2013;48:973–81.
[12] Landis JR, Koch GG. The measurement of observer agreement for categorical data. Biometrics 1977;33:159–74.
[13] Yamaguchi K, Enjoji M. Adenosquamous carcinoma of the pancreas: a clinicopathologic study. J Surg Oncol 1991;47:109–16.
[14] Murakami Y, Yokoyama T, Yokoyama Y, Kanehiro T, Uemura K, Sasaki M, et al. Adenosquamous carcinoma of the pancreas: preoperative diagnosis and molecular alterations. J Gastroenterol 2003;38:1171–5.
[15] Hsu JT, Yeh CN, Chen YR, Chen HM, Hwang TL, Jan YY, et al. Adenosquamous carcinoma of the pancreas. Digestion 2005;72:104–8.
[16] Klöppel G, Hruban RH, Longnecker DS, Adler G, Kern SE, Partanen TJ. Ductal adenocarcinoma of the pancreas. In: Hamilton SR, Aaltonen LA, editors. World Health Organization classification of tumours pathology and genetics of tumours of the digestive system. Lyon: IARC Press; 2000. pp. 221–30.
[17] Klimstra DS, Arnold R, Capella C, Hruban RH, Klöppel G. Neuroendocrine neoplasms of the pancreas. In: Bosman FT, Carneiro F, Hruban RH, Theise ND,

editors. WHO classification of tumours of the digestive system. 4th ed. Lyon, France: IARC Press; 2010. pp. 322–6.
[18] Klimstra DS, Hruban RH, Klöppel G, Morohoshi T, Ohike N. Acinar cell neoplasms of the pancreas. In: Bosman FT, Carneiro F, Hruban RH, Theise ND, editors. WHO classification of tumours of the digestive system. 4th ed. Lyon, France: IARC Press; 2010. pp. 314–21.
[19] Holen KD, Klimstra DS, Hummer A, Gonen M, Conlon K, Brennan M, et al. Clinical characteristics and outcomes from an institutional series of acinar cell carcinoma of the pancreas and related tumors. J Clin Oncol 2002;20:4673–8.
[20] Moore MJ, Goldstein D, Hamm J, Figer A, Hecht JR, Gallinger S, et al. Erlotinib plus gemcitabine compared with gemcitabine alone in patients with advanced pancreatic cancer: a phase III trial of the National Cancer Institute of Canada Clinical Trials Group. J Clin Oncol 2007;25:1960–6.
[21] Conroy T, Desseigne F, Ychou M, Bouche O, Guimbaud R, Becouarn Y, et al. FOLFIRINOX versus gemcitabine for metastatic pancreatic cancer. N Engl J Med 2011;364:1817–25.
[22] Agarwal B, Abu-Hamda E, Molke KL, Correa AM, Ho L. Endoscopic ultrasound-guided fine needle aspiration and multidetector spiral CT in the diagnosis of pancreatic cancer. Am J Gastroenterol 2004;99:844–50.
[23] DeWitt J, Devereaux B, Chriswell M, McGreevy K, Howard T, Imperiale TF, et al. Comparison of endoscopic ultrasonography and multidetector computed tomography for detecting and staging pancreatic cancer. Ann Intern Med 2004;141:753–63.
[24] Palazzo L, Roseau G, Gayet B, Vilgrain V, Belghiti J, Fekete F, et al. Endoscopic ultrasonography in the diagnosis and staging of pancreatic adenocarcinoma. Results of a prospective study with comparison to ultrasonography and CT scan. Endoscopy 1993;25:143–50.
[25] Muller MF, Meyenberger C, Bertschinger P, Schaer R, Marincek B. Pancreatic tumors: evaluation with endoscopic US, CT, and MR imaging. Radiology 1994;190:745–51.
[26] Soriano A, Castells A, Ayuso C, Ayuso JR, de Caralt MT, Gines MA, et al. Preoperative staging and tumor resectability assessment of pancreatic cancer: prospective study comparing endoscopic ultrasonography, helical computed tomography, magnetic resonance imaging, and angiography. Am J Gastroenterol 2004;99:492–501.
[27] Tierney WM, Francis IR, Eckhauser F, Elta G, Nostrant TT, Scheiman JM. The accuracy of EUS and helical CT in the assessment of vascular invasion by peripapillary malignancy. Gastrointest Endosc 2001;53:182–8.
[28] Wallace MB, Hawes RH, Durkalski V, Chak A, Mallery S, Catalano MF, et al. The reliability of EUS for the diagnosis of chronic pancreatitis: interobserver agreement among experienced endosonographers. Gastrointest Endosc 2001;53:294–9.
[29] Topazian M, Enders F, Kimmey M, Brand R, Chak A, Clain J, et al. Interobserver agreement for EUS findings in familial pancreatic-cancer kindreds. Gastrointest Endosc 2007;66:62–7.
[30] Gangi S, Fletcher JG, Nathan MA, Christensen JA, Harmsen WS, Crownhart BS, et al. Time interval between abnormalities seen on CT and the clinical diagnosis of pancreatic cancer: retrospective review of CT scans obtained before diagnosis. AJR Am J Roentgenol 2004;182:897–903.

J Gastroenterol
DOI 10.1007/s00535-014-0987-2

The Japanese Society of Gastroenterology

Does the WHO 2010 classification of pancreatic neuroendocrine neoplasms accurately characterize pancreatic neuroendocrine carcinomas?

Susumu Hijioka · Waki Hosoda · Nobumasa Mizuno · Kazuo Hara · Hiroshi Imaoka · Vikram Bhatia · Mohamed A. Mekky · Masahiro Tajika · Tsutomu Tanaka · Makoto Ishihara · Tatsuji Yogi · Hideharu Tsutumi · Toshihisa Fujiyoshi · Takamitsu Sato · Nobuhiro Hieda · Tsukasa Yoshida · Nozomi Okuno · Yasuhiro Shimizu · Yasushi Yatabe · Yasumasa Niwa · Kenji Yamao

Received: 21 May 2014 / Accepted: 31 July 2014

Abstract
Background The WHO classified pancreatic neuroendocrine neoplasms in 2010 as G1, G2, and neuroendocrine carcinoma (NEC), according to the Ki67 labeling index (LI). However, the clinical behavior of NEC is still not fully studied. We aimed to clarify the clinicopathological and molecular characteristics of NECs.
Methods We retrospectively evaluated the clinicopathological characteristics, *KRAS* mutation status, treatment response, and the overall survival of eleven pNEC patients diagnosed between 2001 and 2014 according to the WHO 2010. We subclassified WHO-NECs into well-differentiated NEC (WDNEC) and poorly differentiated NEC (PDNEC). The latter was further subdivided into large-cell and small-cell subtypes.
Results The median Ki67 LI was 69.1 % (range 40–95 %). Eleven WHO-NECs were subclassified into 4 WDNECs and 7 PDNECs. The latter was further separated into 3 large-cell and 4 small-cell subtypes. Comparisons of WDNEC vs. PDNEC revealed the following traits: hypervascularity on CT, 50 % (2/4) vs. 0 % (0/7) ($P = 0.109$); median Ki67 LI, 46.3 % (40–53 %) vs. 85 % (54–95 %) ($P = 0.001$); Rb immunopositivity, 100 % (4/4) vs. 14 % (1/7) ($P = 0.015$); *KRAS* mutations, 0 % (0/4) vs. 86 % (6/7) ($P = 0.015$); response rates to platinum-based chemotherapy, 0 % (0/2) vs. 100 % (4/4) ($P = 0.067$), and median survival, 227 vs. 186 days ($P = 0.227$).
Conclusions The WHO-NEC category may be composed of heterogeneous disease entities, namely WDNEC and PDNEC. These subgroups tended to exhibit differing profiles of Ki67 LI, Rb immunopositivity and *KRAS* mutation, and distinct response to chemotherapy. Further studies for the reevaluation of the current WHO 2010 classification are warranted.

Keywords Neuroendocrine carcinoma · Ki67 labeling index · *KRAS* mutation · WHO classification

Abbreviations

NEN	Neuroendocrine neoplasm
WHO	World Health Organization

S. Hijioka and W. Hosoda contributed equally to this work.

Electronic supplementary material The online version of this article (doi:10.1007/s00535-014-0987-2) contains supplementary material, which is available to authorized users.

S. Hijioka (✉) · N. Mizuno · K. Hara · H. Imaoka · T. Yogi · H. Tsutumi · T. Fujiyoshi · T. Sato · N. Hieda · T. Yoshida · N. Okuno · K. Yamao
Department of Gastroenterology, Aichi Cancer Center Hospital, 1-1 Kanokoden, Chikusa-ku, Nagoya 464-8681, Japan
e-mail: rizasusu@aichi-cc.jp

W. Hosoda · Y. Yatabe
Department of Pathology and Molecular Diagnostics, Aichi Cancer Center Hospital, Nagoya, Japan

V. Bhatia
Department of Medical Hepatology, Institute of Liver and Biliary Sciences, Delhi, India

M. A. Mekky
Department of Tropical Medicine and Gastroenterology, Assiut University Hospital, Assiut, Egypt

M. Tajika · T. Tanaka · M. Ishihara · Y. Niwa
Department of Endoscopy, Aichi Cancer Center Hospital, Nagoya, Japan

Y. Shimizu
Department of Surgery, Aichi Cancer Center Hospital, Nagoya, Japan

Published online: 21 August 2014

NET	Neuroendocrine tumor
NEC	Neuroendocrine carcinoma
EUS-FNA	Endoscopic ultrasound-guided fine needle aspiration
ENETS	European Neuroendocrine Tumor Society
IHC	Immunohistochemistry
PCR	Polymerase chain reaction
SD	Standard deviation
LCNEC	Large-cell NEC
SCNEC	Small cell-NEC
PDAC	Pancreatic ductal adenocarcinoma

Introduction

Ki67 is a powerful prognostic marker of pancreatic neuroendocrine neoplasms (pNENs) [1] and, accordingly, the remarkable revision was made from the former 2000 World Health Organization (WHO) classification system to the current WHO 2010 terminology system, in which mitotic count and/or Ki67 labeling index (LI) were adopted as the pivotal indicator of stratification [2]. NENs are now to be categorized into neuroendocrine tumor (NET)-G1, NET-G2, and neuroendocrine carcinoma (NEC). Whereas NETs-G1/G2 are invariably composed of tumor cells with well-differentiated morphology, NECs usually have poorly differentiated histology with Ki67 LI > 20 % [2, 3]. Accordingly, all NENs with Ki67 LI > 20 % are defined as NEC. Clinically, these tumors are treated with the same platinum-based chemotherapy regimens as small-cell lung cancers [4–6]. However, some reports have recently indicated that a proportion of well-differentiated NENs might have proliferative rates above the threshold for NET-G2 [7, 8]. In addition, the Nordic NEC study reported that patients with a Ki67 <55 % had low responses to platinum-based chemotherapy [9]. We suppose that the current NEC category, as defined by the WHO 2010 classification (WHO-NEC), includes two groups that differ in clinical behaviors as well as pathological characteristics. Information about the clinicopathological features of WHO-NEC group is scant [7–10]. Therefore, we aimed to further characterize the WHO-NEC group in terms of pathological findings, molecular characteristics, and clinical behaviors.

Patients and methods

Patients

We retrospectively retrieved all of the pNENs diagnosed between January 2001 and March 2014 from our hospital database. All patients were recategorized as NET-G1, NET-G2, or NEC according to the WHO 2010 classification. Specimens for histological examination were obtained from preoperative endoscopic ultrasound-guided fine needle aspiration (EUS-FNA), biopsy, and/or surgical resection. All patients diagnosed with small-cell carcinoma were subsequently assessed by contrast enhanced (CE) chest MDCT to exclude the possibility of metastasis from a primary lung cancer [11]. This study was approved by our institutional review board.

Diagnostic and prognostic characterization

The following features were recorded for all patients: age, gender, symptoms, hormonal syndromes, primary and metastatic locations, European Neuroendocrine Tumor Society (ENETS) TNM stage [12], and CE-MDCT features such as anatomical location, tumor size, and contrast enhancement. We recorded the details of all treatments administered to the patients, particularly platinum-based chemotherapy [4, 5, 13].

Endoscopic ultrasound-guided fine needle aspiration (EUS-FNA) and sample preparation

EUS-FNA procedures were performed using a convex linear-array echoendoscope (GF-UGT240 or GF-UCT260; Olympus Optical Co Ltd, Tokyo, Japan) paired with an ultrasound machine (SSD5500 or Prosound α10; Aloka, Tokyo, Japan). We used 22-gauge needles (NA-11J-KBor NA-200H-8022; Olympus Medical System Corp. Ltd., Tokyo, Japan or EchoTip-Ultra Needle; Cook Endoscopy Inc., Winston Salem, N.C., USA or Expect; Boston Scientific Japan, Tokyo, Japan).

Aspirated materials were divided for cytopathological evaluation, cell-block preparation, and *KRAS* mutation analysis. In all patients, specimen adequacy was evaluated on-site by Diff Quick staining (Diff-Quik; Kokusai Shiyaku, Kobe, Japan) by a cytopathologist or cytotechnologist. Cell-blocks were prepared after the fresh specimens were immediately fixed in 10 % formalin and embedded in paraffin. Sliced sections then were stained by hematoxylin and eosin, as well as by immunohistochemical staining (IHC) [14].

Histological evaluation

We defined tumors as NEC that showed diffuse expression of neuroendocrine markers and Ki67 LI of more than 20 %. In accordance with the 2010 WHO classification, tumors characterized by high-grade cytological atypia, apparent pleomorphism, extensive necrosis, and prominent mitotic activity were categorized into poorly differentiated NEC

(PDNEC). Of PDNECs, tumors characterized by diffuse growth of highly atypical cells with small-sized to medium-sized nuclei, finely granular chromatin, and inconspicuous nucleoli, were categorized as small-cell NEC (SCNEC). Carcinomas with large nuclei, coarse chromatin and well-visible nucleoli with nested proliferation were categorized as large-cell NEC (LCNEC). Furthermore, we attempted to extract those tumors whose cytological features were blander than that of PDNEC and rather similar to NET-G2; that is, tumors composed predominantly of cells with low nucleocytoplasmic ratio and small-sized to medium-sized, ovoid nuclei, growing with minimal pleomorphism, and lacking extensive necrosis. We designated these tumors as 'well differentiated NEC (WDNEC)', and separated them from SCNECs and LCNECs. All slides were reviewed and reclassified by the same pathologist (WH).

Immunohistochemistry and Ki67 labeling index

IHC was performed using monoclonal antibodies for chromogranin A (clone SP12, rabbit, 1:200, Neo Markers), synaptophysin (clone SP11, rabbit, 1:100, Neo Markers, Fremont, CA, USA), Ki67 (clone SP6, rabbit, 1:200; Neo Markers), and Rb (clone 3H9, mouse, 1:300; MBL).

The measurement of Ki67 LI was performed under the assistance of digital pathology technology. Briefly, slides were digitally scanned using a Scan Scope XT (Aperio Technologies, Vista, CA, USA). All sections were reviewed to exclude portions with extensive desmoplasia, necrosis and regions with bleeding. The ultimate Ki67 LI was determined as the highest value found in each specimen using the IHC Nuclear Image Analysis tool (Aperio Technologies, Vista, CA, USA) and was similarly measured and determined in cell-block sections of EUS-FNA specimens as described previously [15].

The prominent concern about EUS-FNA is whether WHO classification (grading) is possible with the biopsy specimens. We previously reported a study [15] about a comparison of grades of pNENs between resected and EUS-FNA specimens by Ki67 immunostaining. The concordance rate rose to 90 % when EUS-FNA samples contained more than 2000 neoplastic cells. In accordance with our previous study, we defined the cases whose neoplastic cells were insufficient for grading (less than 2000 cells) as tumors of 'uncertain' grade.

Analysis of KRAS mutation

Genetic analysis was performed on either the fresh specimens or formalin-fixed paraffin-embedded sections. After nucleic acids were extracted and amplified by polymerase chain reaction, gene mutations were analyzed by ABI PRISM 310 Genetic Analyzer (Applied Biosystems) or the Cycleave PCR assay (Takara Co., Ltd); the detail of which was described previously [16, 17].

Statistical analysis

Statistical analysis was performed using SPSS 17.0 (SPSS Inc., Chicago, IL, USA) software and P values <0.05 were considered statistically significant. Categorical variables are expressed as absolute (n) and relative (%) frequencies and were compared using the Chi squared test or Fisher's exact test. Survival was analyzed using the Kaplan–Meier method with the log-rank test.

Results

Ninety-five patients were diagnosed with pNEN at our hospital during the study period. As to grading of pNENs, the WHO classification 2010 suggests two parameters (mitotic count and Ki67 LI) to evaluate the proliferative activity of tumors. We performed grading of pNENs by measuring Ki67 LI and did not employ the mitotic count method, because our study consisted mostly of tumors diagnosed by FNA specimens, which were too small an amount to secure 50 microscopic fields necessary for the calculation of mitotic count. The pNENs were reclassified into uncertain for Ki67 LI ($n = 8$), NET-G1 ($n = 55$), NET-G2 ($n = 21$), and WHO-NEC ($n = 11$) in accordance with the WHO 2010 classification. The 11 cases of WHO-NEC were the subject of analysis in this study (Fig. 1).

Basic demographic and clinical features of patients with WHO-NEC (Tables 1, 2)

Ten (91 %) of 11 patients were symptomatic, mainly with abdominal pain. The median tumor size was 35 mm (range 20–55 mm). Tumors were located in the head, body, and tail of the pancreas in 2, 5, and 4 patients, respectively. Eight (72 %) patients had liver metastasis at the time of diagnosis, two were treated with surgery (ENETS stageIIb and IIIb) and six who received platinum-based chemotherapy (3 cases were cisplatin + irinotecan and 3 cases were cisplatin + etoposide) had a response rate of 67 %. In the remaining 2 patients, one patient received Gemcitabine (case 3) and another patient received Everolimus because we defined it as WDNEC (case 9). The overall median survival was 314 days (range 60–1202 days).

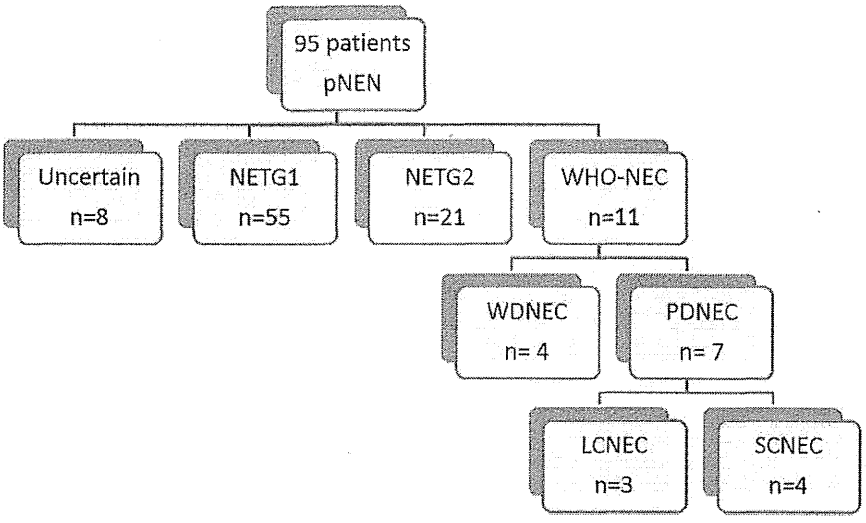

Fig. 1 Algorithm for patient selection from pNEN. *NEN* neuroendocrine neoplasm, *NET* neuroendocrine tumor, *LCNEC* large cell NEC, *SCNEC* small cell NEC, *WDNEC* well-differentiated neuroendocrine carcinoma, *PDNEC* poorly-differentiated neuroendocrine carcinoma

Table 1 Patient characteristics ($n = 11$)

Gender	
Male/female	6/5
Age	
Median (range)	59 years (28–74)
Symptom	
Yes (%)	91 % (abdominal pain)
Site of pancreas tumor	
Head/body/tail	2/5/4
Tumor size	
Median (range)	35 mm (20–55)
Metastasis	
Yes (%)	72 % (liver metastasis)
Treatment	
Operation/chemotherapy/BSC	2/8/1

Imaging features of WHO-NEC on CE-MDCT (Fig. 2; Supplementary Table)

Assessment by CE-MDCT revealed that 9 (82 %) of 11 WHO-NEC in the pancreas were hypovascular. Eight of these tumors had metastasized to the liver, where 7 (88 %) of them were also hypovascular, like the primary tumor (Fig. 2). Before biopsy confirmation, NEN were suspected in only two patients, and the imaging features in the remaining 9 (82 %), suggested pancreatic ductal adenocarcinoma (PDAC). The main pancreatic duct was dilated in 4 (57 %) of 7 patients with tumors located in the head and body of the pancreas.

Pathological and molecular characteristics of WHO-NEC (Fig. 3, Supplementary Figure; Tables 2, 3)

A total of 11 WHO-NEC cases were submitted to the pathological and molecular analysis. No ductal carcinoma components were noted. All cases showed diffuse and strong immunoreactivity for neuroendocrine markers except 1 case, in which only synaptophysin was positive. In total, chromogranin A was expressed in 91 % and synaptophysin was expressed in 100 % of cases. The median Ki67 LI was 69.1 % (range 40–95 %). Nuclear expression of Rb protein was retained in 5 (45 %) tumors. *KRAS* mutations were detected in 6 (55 %) tumors. Seven (64 %) and 4 (36 %) of 11 tumors were categorized as PDNEC (4 SCNECs and 3 LCNECs) and WDNEC, respectively, according to their morphologic characteristics that we mentioned in the "Patients and methods" (Fig. 3, Supplementary Figure).

Clinicopathological comparison of well-differentiated and poorly differentiated NEC (Table 4)

The clinicopathological comparison between the WDNEC and PDNEC groups revealed that they were clinically and molecularly different in several aspects as follows: hypervascularity in MDCT images, 50 % (2/4) vs. 0 % (0/7), $P = 0.109$; median Ki67 LI, 46 % (range 40–53 %) vs. 85 % (range 54–95 %), $P = 0.001$; nuclear expression of Rb, 100 % (4/4) vs. 14 % (1/7), $P = 0.015$; *KRAS* mutations, 0 % (0/4) vs. 86 % (6/7), $P = 0.015$; response rates to platinum-based chemotherapy, 0 % (0/2) vs. 100 % (4/4) $P = 0.067$; and median survival, 227 vs. 186 days, $P = 0.227$.

Table 2 Clinical, pathological features, treatment and response for chemotherapy of WHO-NEC patients

Case	Age/ sex	Location	Size (mm)	ENETS stage	Tissue sampling	Histology	Ki67 LI (%)	CGA	Synaptophysin	Rb	*KRAS*	Treatment	Response for platinum-based regimen
1	30, M	Body	45	IIb	Biopsy and surgical resection	WDNEC	40	Positive	Positive	Positive	WT	Operation	ND
2	59, F	Body	30	IIIb	Biopsy and surgical resection	PDNEC (small cell)	80	Positive	Positive	Positive	MT	Operation	ND
3	49, F	Body	35	IV	Biopsy	PDNEC (large cell)	85	Positive	Positive	Negative	MT	CT (Gemcitabine)	ND
4	68, F	Tail	36	IV	Biopsy	WDNEC	48	Positive	Positive	Positive	WT	CT (IP)	PD
5	63, F	Body	33	IV	Biopsy	PDNEC (large cell)	54	Positive	Positive	Negative	MT	CT (IP)	PR
6	61, M	Body	45	IV	Biopsy	PDNEC (large cell)	90	Positive	Positive	Negative	MT	CT (EP)	PR
7	74, M	Head	20	IV	Biopsy	PDNEC (small cell)	90	Positive	Positive	Negative	WT	BSC	ND
8	37, M	Head	20	IV	Biopsy	PDNEC (small cell)	80	Positive	Positive	Negative	MT	CT (EP)	PR
9	50, F	Tail	35	IV	Biopsy	WDNEC	45	Negative	Positive	Positive	WT	CT (Everolimus)	ND
10	55, M	Tail	30	IV	Biopsy	WDNEC	53	Positive	Positive	Positive	WT	CT (EP)	PD
11	66, M	Tail	70	IV	Biopsy	PDNEC (small cell)	95	Positive	Positive	Negative	MT	CT (IP)	PR

CGA chromogranin A, *WT* wild type, *MT* mutant, *CT* chemotherapy, *IP* cisplatin + irinotecan, *EP* cisplatin + etoposide, *BSC* best supportive care, *ND* not done, *PD* progressive disease, *PR* partial response

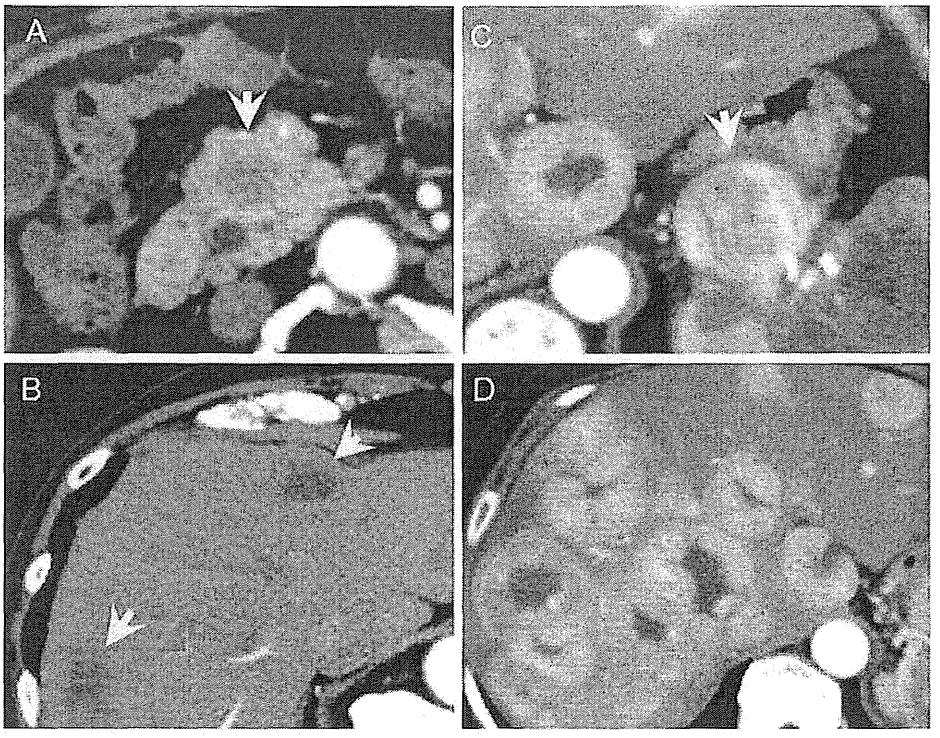

Fig. 2 Computed tomography findings of respective pNECs. **a**, **b** Hypovascular lesions both primary pancreas head site and multiple liver lesions (SCNEC case). **c**, **d** Hypervascular lesions both primary pancreas head site and multiple liver lesions (WDNEC case)

Discussion

When the WHO 2010 classification was applied to our patients with NENs of the pancreas, we found that 36 % of the high-grade category included tumors with well differentiated morphology. This critical finding has an impact on the treatment strategies, particularly the platinum-based chemotherapy which should be originally administered for only PDNEC.

Our findings suggested that WDNECs differ from PDNECs and are rather more closely related to NETs-G2 in terms of clinicopathological and molecular characteristics. Firstly, MDCT consistently showed hypervascularity in WDNEC, but not in PDNEC. Some reports indicated that tumor vascularity correlated with the proliferation index and/or WHO classification [18, 19]. Our findings indicated that only 18 % of WHO-NEC cases were suspected of pNEN according to imaging findings before EUS-FNA, with most being considered PDAC or pancreatic adeno-squamous carcinoma. That is, a significant proportion (82 %) of NECs could not be correctly diagnosed by imaging, especially the PDNEC type.

Histologically, WDNECs shared more morphological traits with NETs-G2 than PDNECs, allowing us to presume that WDNECs correspond to well-differentiated NETs with high proliferative activity. The Ki67 LI tended to be lower in WDNEC than in PDNEC. Notably, *KRAS* and *Rb* genes are promising molecular markers with which to distinguish these types of tumors. The result that *KRAS* mutations were not found in WDNECs supports the notion that this category lies in close proximity to NET-G2, as no pancreatic NETs-G1/G2 have been reported to possess *KRAS* mutations, whereas PDNECs have been shown to harbor *KRAS* mutations [10, 16, 20]. Loss of expression of Rb was found in 86 % of PDNEC cases, whereas all of the WDNEC cases retained its expression. Aberration of the Rb/p16 pathway has been reported to be frequently involved in PDNECs of the pancreas, gallbladder, and ampulla, but not in pancreatic well-differentiated NETs [10, 20–22]. Concerning pancreatic NEN, Yachida et al. [10] conducted immunohistochemical and genetic analyses of several oncogenes and tumor suppressor genes including *KRAS* and *Rb*, and revealed that the aberrations of both genes were common in PDNECs but none in NETs-G1/G2. Their conclusion that PDNECs were molecularly distinct from well-differentiated NETs is in keeping with our findings. Taken together, the difference between WDNEC and PDNEC appears to be clinically, histologically, and molecularly significant, and we consider that WDNECs are more likely to be in the category of well-differentiated NET rather than NEC, thus, favoring the designation, namely "NET-G3".

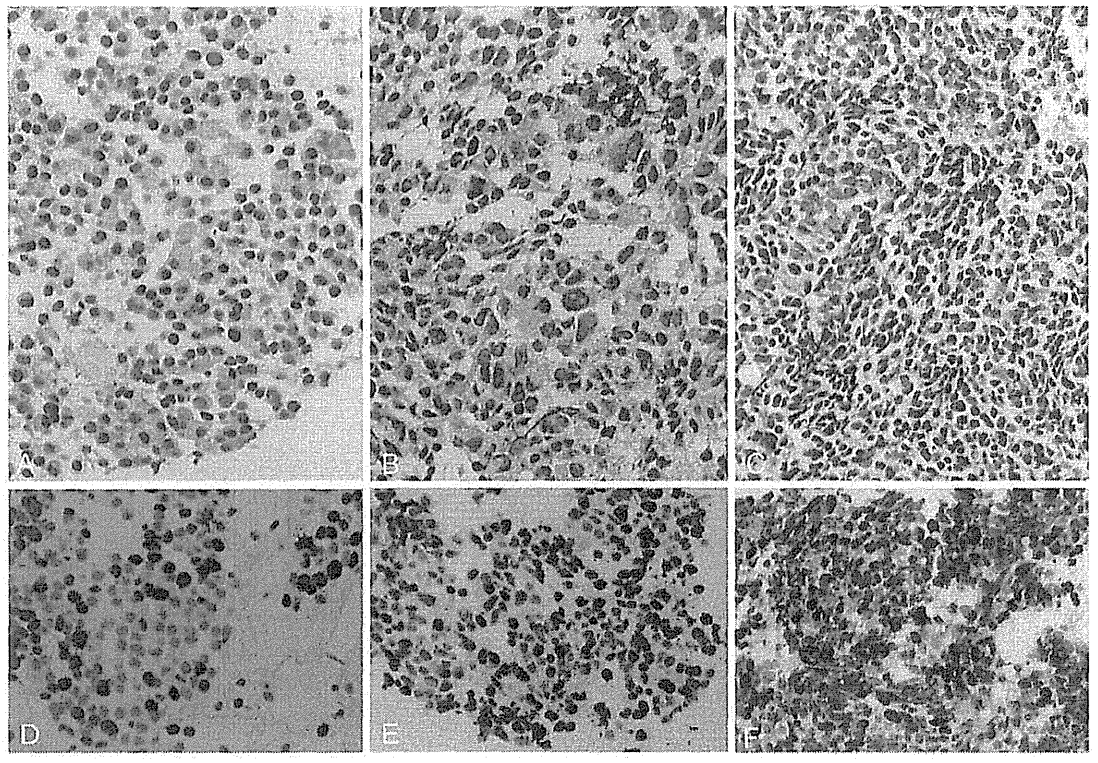

Fig. 3 Histologic features of NECs of the pancreas [H&E stain (**a–c**), and Ki67 (**d–f**), respectively]. The *left column* (**a**, **d**) is a case of WDNEC, the *middle column* (**b**, **e**) is of LCNEC, and the *right column* (**c**, **f**) is of SCNEC. Morphology of WDNECs shows a close similarity to that of NET-G1/G2, characterized by monomorphic growth of tumor cells with highly preserved endocrine cell features. Although LCNECs have features of endocrine cells as well, they are distinguished from WDNECs by increased nuclear atypia, cellular pleomorphism, and the frequent presence of tumor necrosis. SCNECs are composed of small cells with dense chromatin, scarce cytoplasm, and remarkable mitotic activity. These are reminiscent of small cell carcinomas of the lung

Table 3 Pathological and molecular characteristics of WHO-NEC

Ki67 labeling index	
Median (range)	69.1 % (40–95 %)
Morphology	
WDNEC/PDNEC	4/7
Subtypes of PDNEC	
Large-cell type/small-cell type	3/4
Rb immunopositivity	45 % (5/11)
KRAS mutation	54 % (6/11)

WDNEC well-differentiated NEC, *PDNEC* poorly differentiated NEC

Table 4 Clinicopathological comparison of WDNEC and PDNEC

	WDNEC ($n = 4$)	PDNEC ($n = 7$)
Vascularity in pancreas tumor		
Yes (%)	50 % (2/4)	0 % (0/7)
Ki67 labeling index		
Median (range)	46.3 % (40–53 %)	85 % (54–95 %)
Rb immunopositivity	100 % (4/4)	14 % (1/7)
KRAS mutation	0 % (0/4)	86 % (6/7)
Response rate of platinum-based regimen	0 % (0/2)	100 % (4/4)
Prognosis		
Median	227 days	186 days

WDNEC well-differentiated NEC, *PDNEC* poorly differentiated NEC

Our study showed that both WDNEC and PDNEC patients harbored unfavorable outcome (median overall survival of 227 days and 186 days, respectively), which is in stark contrast to NET-G2 patients whose median overall survival is reportedly 162 months [1]. Although WDNEC and PDNEC shared aggressiveness clinically and pathologically, the efficacy of the treatment between them tended to be different; all WDNEC cases did not exhibit response to the platinum-based chemotherapy while all of the PDNEC cases did. The Nordic NEC study [9] found that WHO-NEC with Ki67 LI > 55 % responded to platinum-based chemotherapy, whereas those with Ki67 LI < 55 % did not. Although the Nordic NEC study mainly focused on the treatment and prognostic aspects, there was no detailed description of the pathologic

characteristics of the cases. We suppose that some of their WHO-NEC included WDNEC as defined herein. Based on the results of the Nordic NEC study, the NCCN guidelines noted in footnotes that "intermediate Ki67 levels in the 20–50 % range may not respond well to platinum/etoposide as patients with small cell histology or extremely high Ki67 and so, a clinical judgment should be used". When NEN is diagnosed as WHO-NEC, clinically the toxic platinum-based chemotherapy is usually administered as a first-line regimen. However, a recent case report showed a good response of high-grade NET to molecular targeted therapy with agents such as Everolimus [23]. In fact, one patient who was diagnosed with WDNEC and received Everolimus obtained partial response. The current WHO 2010 classification might be flawed in terms of the management of patients with NEC and the classification scheme for NECs should be revised as the clinical, pathological, and molecular characteristics of this high-grade NEN become more fully clarified.

In regard to IHC, chromogranin A was expressed in 91 % of WHO-NEC cases, and synaptophysin was expressed in 100 %. In a similar fashion, previous articles reported that chromogranin A was expressed in 81–94 %, and synaptophysin was expressed in 88–96 % [7–9]. Taken together, stainability of chromogranin A and synaptophysin is high not only in WDNEC but also in PDNEC.

In our institute, we perform EUS-FNA for the diagnosis of pancreatic tumors on a routine basis, and have been reported its usefulness so far [11, 14–16, 24]. The diagnostic accuracy of overall pancreatic tumors was 91.8 % (918/996) [14]. We previously detected *KRAS* mutations in 87 % (266/307) of EUS-FNA specimens from pancreatic masses in patients with PDAC [24] and none among 25 well-differentiated endocrine tumors [16]. Jiao et al. [20] also reported the absence of *KRAS* mutations in NET-G1/G2.

To the best of our knowledge, this is the first study which examined the clinicopathological characteristics of pNECs, with an emphasis on the difference between WDNEC and PDNEC. However, some limitations should be addressed. The retrospective design hindered precise analysis of all required data, imposed potential selection bias, and the patient cohort was small due to the natural rarity of pNECs that account for <1 % of all pancreatic carcinomas, and 2–7.5 % of all pNEN [2, 25]. Intratumoral heterogeneity is another important consideration. In our 11 cases of NEC, we did not note any adenocarcinoma component histologically nor immunohistochemically. Also, the result of the high frequency of Rb aberration in our series minimizes the possibility of a hidden presence of concomitant adenocarcinomas, as Rb aberration has been reported to be a rare event in PDACs (5–6 %) [26, 27]. Although the above observations do not fully rule out the possibility that some of the cases might contain an accompanying adenocarcinoma, this may be a relatively uncommon occurrence given the low frequency of an associated ductal adenocarcinoma in PDNECs reported by Basturk et al. [8] (6/44, 14 %). Finally, we address the feasibility of grading for pNENs diagnosed by FNA specimens, which constituted most of our series. Past studies of ours and of others claimed that grading by Ki67 LI can be applicable to FNA specimens by showing high concordance between the grade given by the FNA specimens and that by the corresponding resected specimens (concordance rate 78–90 %) [15, 28–31]. Indeed, downgrading or upgrading between G1 and G2 occurred in a small proportion of cases, but there was no tumor observed among the 5 studies that was graded as G3 by EUS-FNA and was downgraded to G2 by surgical resection. This observation, as well as the poor outcome of the current study, indicates that the admixture of 'overestimated' NETs-G2 in our cohort seemed unlikely to happen.

In conclusion, we identified a significant number of "WDNEC" cases among pNECs that were defined by the current WHO classification system. The clinicopathological and molecular analyses suggested that WDNEC is distinct from PDNEC. Though the number of cases we analyzed was limited, we believe that our scheme of subcategorizing pancreatic NEC showed promise. Further larger-scale studies are warranted to validate our stratification of WHO-NECs, which will facilitate a more personalized treatment of the patients with this rare malignant neoplasm.

Acknowledgments This study was supported by a grant from the Pancreas Research Foundation of Japan and JSPS KAKENHI Grant Number 26461041.

Conflict of interest The authors declare that they have no conflict of interest.

References

1. Pape UF, Jann H, Muller-Nordhorn J, et al. Prognostic relevance of a novel TNM classification system for upper gastroenteropancreatic neuroendocrine tumors. Cancer. 2008;113:256–65.
2. Bosman F, Carneiro F, Hruban RH, et al. WHO classification of tumours of the digestive system. Lyon, France: IARC Press; 2010.
3. Rindi G, Klöppel G, Alhman H, et al. TNM staging of foregut (neuro) endocrine tumors: a consensus proposal including a grading system. Virchows Arch. 2006;449:395–401.
4. Moertel CG, Kvols LK, O'Connell MJ, et al. Treatment of neuroendocrine carcinomas with combined etoposide and cisplatin. Evidence of major therapeutic activity in the anaplastic variants of these neoplasms. Cancer. 1991;68:227–32.
5. Mitry E, Baudin E, Ducreux M, et al. Treatment of poorly differentiated neuroendocrine tumours with etoposide and cisplatin. Br J Cancer. 1999;81:1351–5.

6. Pavel M, Baudin E, Couvelard A, et al. ENETS Consensus Guidelines for the management of patients with liver and other distant metastases from neuroendocrine neoplasms of foregut, midgut, hindgut, and unknown primary. Neuroendocrinology. 2012;95:157–76.
7. Velayoudom-Cephise FL, Duvillard P, Foucan L, et al. Are G3 ENETS neuroendocrine neoplasms heterogeneous? Endoc-Relat Cancer. 2013;20:649–57.
8. Basturk O, Tang L, Hruban RH, et al. Poorly differentiated neuroendocrine carcinomas of the pancreas: a clinicopathologic analysis of 44 cases. Am J Surg Pathol. 2014;38:437–47.
9. Sorbye H, Welin S, Langer SW, et al. Predictive and prognostic factors for treatment and survival in 305 patients with advanced gastrointestinal neuroendocrine carcinoma (WHO G3): the NORDIC NEC study. Ann Oncol: Off J Eur Soc Med Oncol/ESMO. 2013;24:152–60.
10. Yachida S, Vakiani E, White CM, et al. Small cell and large cell neuroendocrine carcinomas of the pancreas are genetically similar and distinct from well-differentiated pancreatic neuroendocrine tumors. Am J Surg Pathol. 2012;36:173–84.
11. Hijioka S, Matsuo K, Mizuno N, et al. Role of endoscopic ultrasound and endoscopic ultrasound-guided fine-needle aspiration in diagnosing metastasis to the pancreas: a tertiary center experience. Pancreatol : Off J Int Assoc Pancreatol. 2011;11:390–8.
12. Rindi G, Kloppel G, Alhman H, et al. TNM staging of foregut (neuro)endocrine tumors: a consensus proposal including a grading system. Virchows Archiv: Int J Pathol. 2006;449:395–401.
13. Plockinger U, Rindi G, Arnold R, et al. Guidelines for the diagnosis and treatment of neuroendocrine gastrointestinal tumours. A consensus statement on behalf of the European Neuroendocrine Tumour Society (ENETS). Neuroendocrinology. 2004;80:394–424.
14. Haba S, Yamao K, Bhatia V, et al. Diagnostic ability and factors affecting accuracy of endoscopic ultrasound-guided fine needle aspiration for pancreatic solid lesions: Japanese large single center experience. J Gastroenterol. 2013;48:973–81.
15. Hasegawa T, Yamao K, Hijioka S, et al. Evaluation of Ki-67 index in EUS-FNA specimens for the assessment of malignancy risk in pancreatic neuroendocrine tumors. Endoscopy. 2014;46:32–8.
16. Hosoda W, Takagi T, Mizuno N, et al. Diagnostic approach to pancreatic tumors with the specimens of endoscopic ultrasound-guided fine needle aspiration. Pathol Int. 2010;60:358–64.
17. Yatabe Y, Hida T, Horio Y, et al. A rapid, sensitive assay to detect EGFR mutation in small biopsy specimens from lung cancer. J Mol Diagn. 2006;8:335–41.
18. Rodallec M, Vilgrain V, Couvelard A, et al. Endocrine pancreatic tumours and helical CT: contrast enhancement is correlated with microvascular density, histoprognostic factors and survival. Pancreatol: Off J Int Assoc Pancreatol. 2006;6:77–85.
19. d'Assignies G, Couvelard A, Bahrami S, et al. Pancreatic endocrine tumors: tumor blood flow assessed with perfusion CT reflects angiogenesis and correlates with prognostic factors1. Radiology. 2009;250:407–16.
20. Jiao Y, Shi C, Edil BH, et al. DAXX/ATRX, MEN1, and mTOR pathway genes are frequently altered in pancreatic neuroendocrine tumors. Science. 2011;331:1199–203.
21. Nassar H, Albores-Saavedra J, Klimstra DS. High-grade neuroendocrine carcinoma of the ampulla of vater: a clinicopathologic and immunohistochemical analysis of 14 cases. Am J Surg Pathol. 2005;29:588–94.
22. Parwani AV, Geradts J, Caspers E, et al. Immunohistochemical and genetic analysis of non-small cell and small cell gallbladder carcinoma and their precursor lesions. Mod Pathol: Off J USA Can Acad Pathol Inc. 2003;16:299–308.
23. Fonseca PJ, Uriol E, Galván JA, et al. Prolonged clinical benefit of Everolimus therapy in the management of high-grade pancreatic neuroendocrine carcinoma. Case Rep Oncol. 2013;6:441–9.
24. Ogura T, Yamao K, Sawaki A, et al. Clinical impact of K-ras mutation analysis in EUS-guided FNA specimens from pancreatic masses. Gastrointest Endosc. 2012;75:769–74.
25. Ito T, Igarashi H, Nakamura K, et al. Epidemiological trends of pancreatic and gastrointestinal neuroendocrine tumors in Japan: a nationwide survey analysis. J Gastroenterol. 2014. doi:10.1007/s00535-014-0934-2.
26. Barton CM, McKie AB, Hogg A, et al. Abnormalities of the RB1 and DCC tumor suppressor genes: uncommon in human pancreatic adenocarcinoma. Mol Carcinog. 1995;13:61–9.
27. Gerdes B, Ramaswamy A, Ziegler A, et al. p16INK4a is a prognostic marker in resected ductal pancreatic cancer: an analysis of p16INK4a, p53, MDM2, an Rb. Ann Surg. 2002;235:51–9.
28. Weynand B, Borbath I, Bernard V, et al. Pancreatic neuroendocrine tumour grading on endoscopic ultrasound-guided fine needle aspiration: high reproducibility and inter-observer agreement of the Ki-67 labelling index. Cytopathology. 2013. doi:10.1111/cyt.12111.
29. Piani C, Franchi GM, Cappelletti C, et al. Cytological Ki-67 in pancreatic endocrine tumours: an opportunity for pre-operative grading. Endocr Relat Cancer. 2008;15:175–81.
30. Larghi A, Capurso G, Carnuccio A, et al. Ki-67 grading of nonfunctioning pancreatic neuroendocrine tumors on histologic samples obtained by EUS-guided fine-needle tissue acquisition: a prospective study. Gastrointest Endosc. 2012;76:570–7.
31. Chatzipantelis P, Konstantinou P, Kaklamanos M, et al. The role of cytomorphology and proliferative activity in predicting biologic behavior of pancreatic neuroendocrine tumors: a study by endoscopic ultrasound-guided fine-needle aspiration cytology. Cancer. 2009;117:211–6.

Can Long-Term Follow-Up Strategies Be Determined Using a Nomogram-Based Prediction Model of Malignancy Among Intraductal Papillary Mucinous Neoplasms of the Pancreas?

Susumu Hijioka, MD, Yasuhiro Shimizu, MD,† Nobumasa Mizuno, MD,* Kazuo Hara, MD,* Hiroshi Imaoka, MD,* Mohamed A. Mekky, MD,‡ Vikram Bhatia, MD,§ Yoshikuni Nagashio, MD,* Toshiyuki Hasegawa, MD,* Akihide Shinagawa, MD,* Masanari Sekine, MD,* Masahiro Tajika, MD,|| Tsutomu Tanaka, MD,|| Makoto Ishihara, MD,|| Yasumasa Niwa, MD,|| and Kenji Yamao, MD**

Objectives: This study investigated whether a risk assessment nomogram can predict the malignant potential of intraductal papillary mucinous neoplasms (IPMNs) and provide valuable information for the follow-up and counseling strategies of such patients.

Methods: We studied 126 of 589 patients with IPMN who were followed up for at least 36 months with annual endoscopic ultrasonography. We analyzed scores derived from our nomogram, incorporating the parameters of sex, lesion type, mural nodule height, and pancreatic juice cytology determined at the initial IPMN evaluation.

Results: The rate of malignant IPMNs was 5.5% (7/126). The initial average nomogram score was 19.8 (range, 0–55), and the final follow-up average was 23.8 (range, 0–109). When a cutoff score was set at 35 points, the sensitivity, specificity, and accuracy of the nomogram to assess malignancy risk were 87.5%, 96.6%, and 96%, respectively. The area under the receiver operating characteristic curve of malignant IPMN prediction during follow-up was 0.865.

Conclusions: The ability of the nomogram to predict malignancy in patients with IPMN was validated. Our findings can suggest that a follow-up for patients at high and low risk for cancer progression could be scheduled every 3 to 6 and 12 months, respectively.

Key Words: IPMN, risk scoring model, treatment, nomogram

(*Pancreas* 2014;43: 367–372)

Ohashi et al[1] originally described intraductal papillary mucinous neoplasms (IPMNs) of the pancreas as mucin-secreting tumors in 1982. The number of individuals diagnosed with IPMN based on the 2005 International Consensus Guidelines for the Management of IPMNs[2] revised in 2012 is increasing.[3] Although IPMNs are considered malignant, clear data that can guide follow-up protocols are not available. The 2012 guidelines recommend a follow-up schedule based on cyst size, namely, annually, every 6 to 12 months, and every 3 to 6 months for cysts that are less than 10 mm, 10 to 20 mm, and more than 20 mm.[3] However, several reports have shown that cyst size alone is not a suitable morphological parameter for evaluating malignancy potential.[4–7] Moreover, a single variable such as cyst size is insufficiently reliable for planning individualized follow-up strategies. Hence, a new risk scoring model is needed to predict the likelihood of carcinoma occurrence and to establish follow-up protocols.

Nomograms are predictive mathematical models that calculate the overall probability based on several factors and are thus more accurate than other models.[8] Treatment and follow-up strategies for various neoplasms such as prostate and colorectal cancers have often been developed based on nomograms.[8–12]

Here, we validate a nomogram that we originally constructed to predict malignancy in 81 patients who had undergone an IPMN resection.[13] The nomogram predicted malignancy with an area under receiver operating characteristic curve (AUC) of 0.903 in that patient set.

In our previous study, multivariate analysis with 81 patients who had undergone IPMN resection demonstrated that pancreatic carcinoma was associated with the female sex, main pancreatic duct (MPD) IPMN, nodule size, and pancreatic juice cytology grade in patients. Thus, the present study performed a retrospective evaluation of whether a scoring system incorporating these variables was a good reflection of the risk for pancreatic carcinoma.

MATERIALS AND METHODS

Patients' Selection

A retrospective study was designed to evaluate our database registry system of endoscopic ultrasonography (EUS) procedures, which revealed 18,000 that were performed between September 1988 and April 2013 at Aichi Cancer Center Hospital (Nagoya, Japan). Of them, we identified 589 patients with IPMN. Among these 589 patients, 126 patients who fulfilled our inclusion criteria were included in the study.

Inclusion Criteria

- Patients had to be followed up for at least 3 years after diagnosis.
- Available data on sex, lesion type, mural nodule (MN) height measured by EUS, and pancreatic juice cytology findings obtained by endoscopic retrograde pancreatography (ERP).
- Patients had to be free of concomitant pancreatic ductal adenocarcinoma development.

The remaining 460 were excluded from the analysis because of the short follow up period (<3 years, n = 372), missing pancreatic juice cytology data (n = 83), or pancreatic ductal adenocarcinoma developing during the study period (n = 3). To avoid a potential for selection bias, 2 patients were also excluded because they were duplicated in our formal study of the original nomogram.

This study was approved by our institutional review board.

From the Departments of *Gastroenterology, and †Gastrointestinal Surgery, Aichi Cancer Center Hospital, Nagoya, Japan; ‡Department of Tropical Medicine and Gastroenterology, Assiut University Hospital, Assiut, Egypt; §Department of Medical Hepatology, Institute of Liver and Biliary Sciences, Delhi, India; and ||Department of Endoscopy, Aichi Cancer Center Hospital, Nagoya, Japan.

Received for publication December 26, 2012; accepted August 6, 2013.

Reprints: Susumu Hijioka, MD, Department of Gastroenterology, Aichi Cancer Center Hospital, 1-1 Kanokoden, Chikusa-ku, Nagoya, Aichi 464-8681, Japan (e-mail: rizasusu@aichi-cc.jp).

The authors declare no conflict of interest.

TABLE 1. Clinical Characteristics of Patients

Factors	Patients (n = 126)
Male/female	70/56
Age, median (range), y	62.3 (33–77)
Period, median (range), mo	89 (36–269)
EUS times, median (range)	6.1 (2–15)
Symptomatic/asymptomatic, n (%)	14/112 (9)
MPD type-BD type ratio	6:120
Nodules, n (%)	Yes, 19 (14.%); no, 107 (89.1)
Nodule size, median (range), mm	3.5 (2–5)
Cytological classification (I/II/III/IV/V)	48/62/16/0/0

Evaluation of IPMN Size

The maximal diameter of MNs as well as the sizes of cysts and the MPD were measured by EUS along with computed to mography (CT) and/or magnetic resonance cholangiopancreatography (MRCP).

Follow-Up Protocol

This is composed of at least an annual evaluation with EUS and laboratory tests plus CT and/or MRCP examination every 12 months.

Indications for Surgery

These included MPDs 10 mm or greater, MNs 5 mm or greater, short-term disease progression with a high likelihood of malignancy, cytological detection of malignant cells in pancreatic juice, and significant symptoms such as acute pancreatitis.

Diagnosis of IPMN

Others have characterized IPMN based on the patulous appearance of the ampulla of Vater, filling defects in the pancreatic duct on ERCP, or cystic lesions connecting with the MPD, as determined by EUS, MRCP, and/or CT imaging. Lesions that predominantly involved the MPD and caused a dilatation 10 mm or greater were classified as MPD-IPMN, whereas those that mainly involved a branch pancreatic duct were classified as branch duct (BD)–IPMN.

Cytopathological Evaluation

Two experienced pathologists (Y.Y. and W.H.) reviewed all resected lesions. Based on the degree of cytoarchitectural atypia and the arrangement of the intraductal components, tumors were classified as IPMN adenoma, borderline IPMN, IPMN carcinoma in situ (noninvasive intraductal papillary mucinous carcinoma [IPMC]), or invasive IPMC in accordance with the World Health Organization classification system.[14]

Nomogram

The nomogram incorporated the following risk factors: sex, lesion type, MN height, and pancreatic juice cytology data according to the logistic regression model. Each predictor was scored between 0 and 100, and the scores were totaled. The sum of all scores was represented on a vertical axis that was used to estimate malignancy risk (Fig. 1). The ability of the nomogram to predict malignancy potential had an AUC of 0.903 in the original patient cohort.[13]

Statistical Analysis

Continuous variables are described as mean (SD), and dichotomous variables are expressed as simple proportions. The χ^2 test was used for comparative analyses. Data were statistically analyzed using the SPSS software for Windows, release 11 (SPSS Inc, Chicago, Ill). Significance was achieved when P is less than 0.05. The optimal cutoff levels for nomogram point were determined by receiver operating characteristic (ROC) curves to differentiate the low-risk group from the high-risk group of developing cancer and identify the point which showed equal sensitivity and specificity, which were also calculated.

RESULTS

Patients' Characteristics

A total of 108 patients with IPMN (male, n = 70; mean age, 62.3 years at the time of diagnosis) were followed up for a

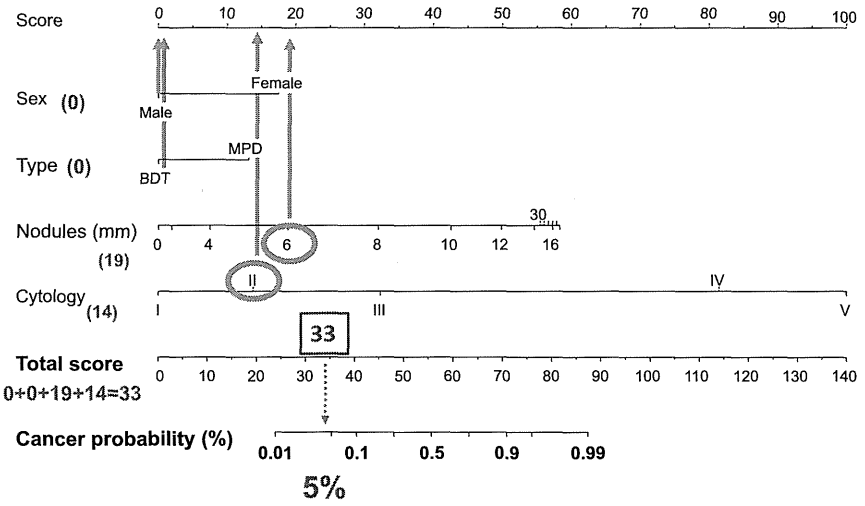

FIGURE 1. How to use the nomogram. Find the position of each variable on the corresponding axis, draw a line to the "points" axis for the number of points, add the points from all variables, and draw a line from the "total points" axis to determine cancer probability at the bottom. For example, for BD-IPMN in men, the nodule height was 6 mm, the cytological classification of the pancreatic juice was class II, men had 0 point, branch duct type was 0 point, 6-mm nodule height corresponds to 19 points, and cytological class II corresponds to 14 points. The total score was 0 + 0 + 19 + 14 = 33, where cancer probability was calculated as approximately 5%. BDT, branch duct type.

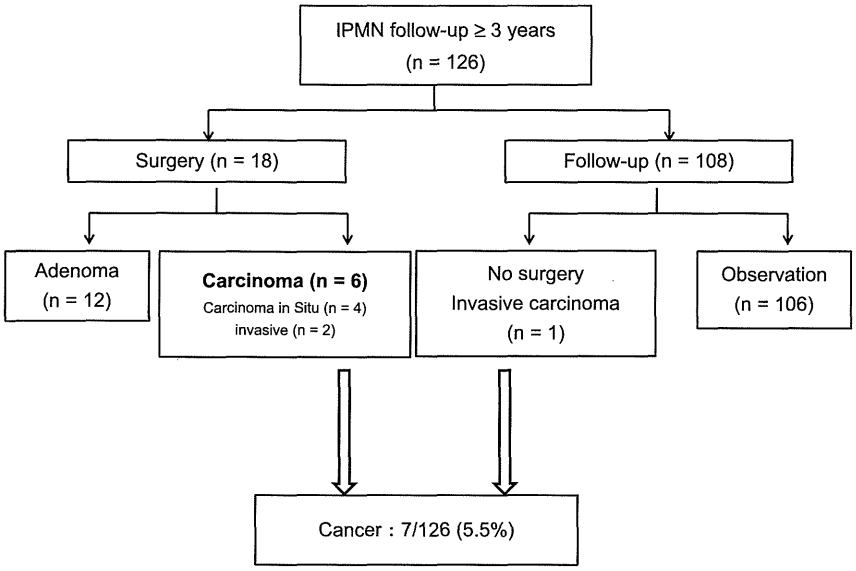

FIGURE 2. Clinical course of IPMN followed up for 3 years or more. Only 5.6% (6/108) of patients developed malignancies, assuming that the entire follow-up group had only benign lesions at the start of study.

median of 89 months (range, 36–269 months). Each patient underwent an average of 6.1 EUS procedures (range, 2–15 procedures) throughout the follow-up period. Six and 120 patients had MPD-IPMN and BD-IPMN, respectively. The median diameters of the cysts and MPDs were 18.6 mm (range, 0–60 mm) and 2.7 mm (range, 1–10 mm), respectively. Nineteen patients (14.9%) had MNs with a median size of 3.5 mm (range, 2–5 mm). Pancreatic juice cytology was classified as I, II, and III in 48, 62, and 16 patients, respectively, among whom 18 (14.2%) underwent surgery. Table 1 summarizes the clinical characteristics of the patients.

Follow-Up Results

Patients were assigned to either a group that was followed up for at least 3 years (follow-up group) or an operation group throughout the follow-up period. The follow-up group included 1 patient who developed carcinoma. This patient was managed with a best supportive care regimen because of having a poor performance status and was excluded thereafter from the analysis. The operation group (n = 18) was composed of patients who had undergone surgery to treat MPD dilation (n = 5), large MNs (n = 9), or acute pancreatitis (n = 4). Among them, 12 had adenoma and 6 had carcinoma (in situ, n = 4; minimally invasive,

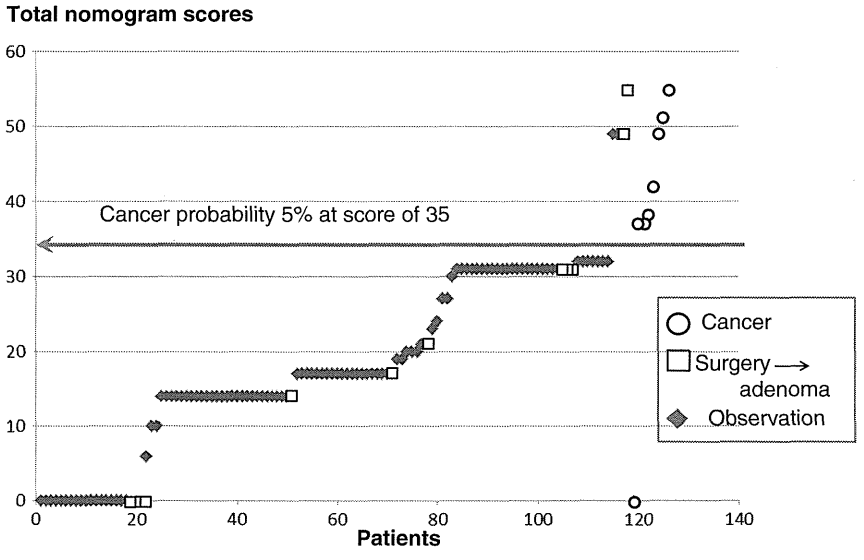

FIGURE 3. Initial nomogram total scores for all patients in order. Diamonds, squares, and circles indicate patients who were observed, underwent surgery to treat adenoma and patients with cancer respectively. A score of 35 indicates a 5% probability of developing cancer.

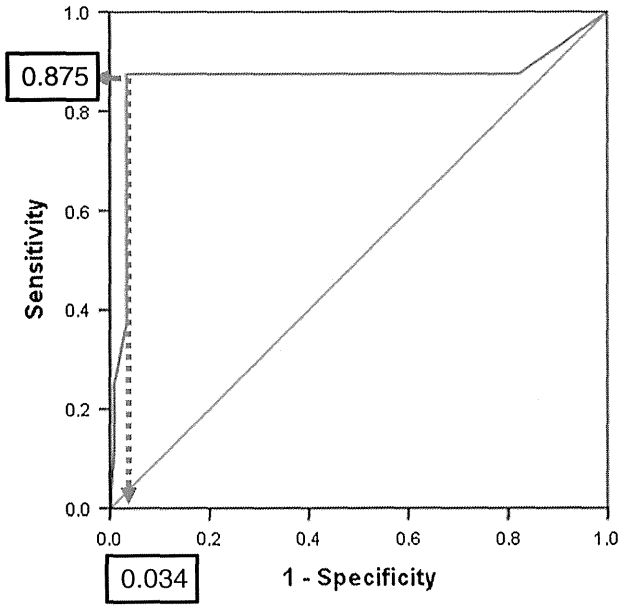

FIGURE 4. ROC analysis of prediction of IPMC during follow-up for IPMN. Area under the ROC curve, 0.865. The optimal cutoff level for nomogram point to differentiate the low-risk group from the high-risk group of developing cancercancer was 35 points. It was determined by the point, which showed equal sensitivity and specificity on the ROC curve. When a score of 35 points was taken as the cutoff, the sensitivity and specificity of the nomogram to assess malignancy risk were 87.5% and 96.6%, respectively.

n = 1; invasive, n = 1). Only 7 (5.5%) of 126 patients developed a malignant disease, assuming that the entire follow-up group had only benign lesions at the start of the study. Figure 2 summarizes these results.

Prediction of Malignant Transformation During Follow-Up

Figure 3 shows the details of all patients (including sex, lesion type, MN height, and pancreatic juice cytology) that were incorporated into our nomogram at the time of the initial presentation. The nomogram predicted IPMCs with an AUC of 0.865 (Fig. 4). The optimal cutoff point based on the ROC curve was at point 35, which was the most appropriate, and the nomogram estimated the cancer risk as 5% with a sensitivity of 87.5% (7/8), a specificity of 96.6% (114/118), a positive predictive value of 63.6% (7/11), a negative predictive value (NPV) of 99.1% (114/115), and an accuracy of 96% (Table 2). One patient with cancer who scored less than 35 points on the nomogram had carcinoma in situ without MNs.

Change of the Nomogram Point

The average score of the initial nomogram was 19.8 (range, 0–55), and the average final follow-up nomogram score was 23.8 (range, 0–109). Figure 5 shows the changing rate of the nomogram of 18 operated cases. The changing rate of 12 adenoma cases was 37.6% ± 41.2% (0%–98%), whereas the changing rate of 6 carcinoma cases were 36.2% ± 32.7% (0%–92.3%), without significant difference (P = 0.939) between the 2 groups.

DISCUSSION

Intraductal papillary mucinous neoplasms are proliferative and mucin-producing epithelial lesions that gradually progress from adenoma to carcinoma in situ and eventually to an invasive carcinoma.[1] Protocols for scheduling resection and follow-up have not been established because the progression profiles of these lesions are unclear. The 2010 consensus agreement recommended developing follow-up strategies based on cyst size,[2,3] but this recommendation remains debatable. Many studies have suggested MN height as the most suitable morphological parameter for assessing malignancy,[4,7,15] whereas others have demonstrated that a large cyst diameter is a sign of malignancy in BD-IPMN.[16–18] In contrast, Sadakari et al[19] reported that 8.2% of IPMNs progress to malignancy despite the absence of MNs. Basing management strategies on a single parameter might be inappropriate, whereas nomograms that take multiple factors into consideration should predict malignant progression more reliably and lead to the development of strategies that are more precisely tailored to the needs of individual patients.

We created a cancer prediction nomogram for patients who have undergone an IPMN resection. This nomogram based on the significant predictive factors of sex, lesion type, nodule height, and pancreatic juice cytology data provided an excellent cancer prediction capability with an AUC of 0.903.[13] Here, we validated this nomogram in a cohort of patients with IPMN who underwent follow-up during a relatively long period (≥3 years) at our institute. The outcome of this study was also excellent (positive predictive value, 63.6%; NPV, 99.1%; accuracy, 96% for development of malignancy) at a cutoff score of 35 that was equivalent to a 5% probability of developing cancer. When we define a score of 35 or higher as high risk and a score of less than 35 as low risk, the low-risk group (scores of <35) indicated an extremely low risk of developing IPMN-derived cancer during the follow-up period of 5 years (NPV, 99.1%) and the high-risk group (scores of >35) indicated a high risk of developing an IPMN-associated carcinoma, with 87.5% of patients having an IPMC at a follow-up of more than 3 years. Based on these results, we recommend a follow-up assessment every 6 months for scores of 35 or higher and annually for those with less than 35, depending on the patient's status. Patients with IPMN are at increased risk not only for cancer derived from these lesions, but also for ductal adenocarcinoma (1.9%–8.0%).[5,6,20–22] Hence, even with low-risk scores of less than 35, we recommend at least an annual follow-up. Notably, one of our patients with a score of 0 at initial testing developed carcinoma in situ without detectable MNs 6 years after the first follow-up. In the present study, ERP cytology was the only method that could detect malignancy for these cases with no MNs. It has also been reported that ERP juice cytology examination alone might be ineffective because of its low sensitivity.[23,24] Therefore, ERP cytology should be augmented with other risk assessment tools such as

TABLE 2. Diagnostic Yield of Nomogram: Benign Versus Malignant

Final Nomogram	Malignant	Benign	Total
Positive (n = 11)	7 (TP)	4 (FP)	11
Negative (n = 115)	1 (FN)	114 (TN)	115
Total	8	118	126

FN indicates false negative; FP, false positive; TN, True negative; TP, true positive.